

Original Research

An integrated Bayesian model for estimating the long-term health effects of air pollution by fusing modelled and measured pollution data: A case study of nitrogen dioxide concentrations in Scotland



Guowen Huang*, Duncan Lee, Marian Scott

School of Mathematics and Statistics, University Gardens, University of Glasgow, Glasgow G12 8QW, UK

ARTICLE INFO

Article history:

Received 10 March 2015

Revised 11 July 2015

Accepted 23 September 2015

Available online 3 October 2015

Keywords:

Air pollution

Health effects

Respiratory disease

Spatio-temporal model

ABSTRACT

The long-term health effects of air pollution can be estimated using a spatio-temporal ecological study, where the disease data are counts of hospital admissions from populations in small areal units at yearly intervals. Spatially representative pollution concentrations for each areal unit are typically estimated by applying Kriging to data from a sparse monitoring network, or by computing averages over grid level concentrations from an atmospheric dispersion model. We propose a novel fusion model for estimating spatially aggregated pollution concentrations using both the modelled and monitored data, and relate these concentrations to respiratory disease in a new study in Scotland between 2007 and 2011.

© 2015 The Authors. Published by Elsevier Ltd. This is an open access article under the CC BY license (<http://creativecommons.org/licenses/by/4.0/>).

1. Introduction

Air pollution is a global health problem, as a recent World Health Organisation report estimates that outdoor air pollution was responsible for the premature deaths of 3.7 million people under the age of 60 in 2012 ([World Health Organisation, 2014](#)). The long-term effects of air pollution can be estimated using cohort or spatio-temporal ecological study designs, with examples of the former including [Pope et al. \(2002\)](#) and [Laden et al. \(2006\)](#). However, such studies are expensive and time consuming to implement, due to the long-term follow up required for the cohort. Therefore spatio-temporal ecological studies are also used (e.g. [Elliott et al., 2007](#); [Lee et al., 2009](#)), as they are easy to implement due to the routine availability of the required data.

They estimate health effects based on geographical and temporal contrasts in air pollution and disease risk across n contiguous small-areas, such as census tracts or electoral wards, for multiple time periods. The disease data are counts of the numbers of disease cases in each areal unit and time period, and thus Poisson log-linear models are typically used for modelling. The covariates include air pollution concentrations and known confounders such as socio-economic deprivation, and are augmented by a set of random effects that account for residual spatio-temporal autocorrelation. The random effects are commonly modelled using Gaussian Markov Random Fields (GMRF) prior distributions within a Bayesian inferential setting, with the special case of conditional autoregressive (CAR, [Besag et al., 1991](#)) priors being commonly used.

One key problem in these studies is estimating spatially representative pollution concentrations, using either measured data from a sparse network of monitors or modelled concentrations on a regular grid from an

* Corresponding author.

E-mail address: g.huang.1@research.gla.ac.uk (G. Huang).

atmospheric dispersion model, such as those produced by AEA (2011). The latter provide complete spatial coverage of the study region but are known to contain biases (Berrocal et al., 2010a). However, the monitored (point locations) and modelled (grid boxes) pollution data are spatially misaligned with the disease data (irregularly shaped areal units), and this problem is often referred to as the *change of support problem* (Gelfand et al., 2001; Gotway and Young, 2002). Geostatistical Kriging has been used to spatially align the monitored pollution data to the disease counts (Elliott et al., 2007; Janes et al., 2007), while simple averaging is used to correct the spatial misalignment of the modelled concentrations (Maheswaran et al., 2006; Lee et al., 2009; Warren et al., 2012). Recently, Vinikoor-Imler et al. (2013), Vinikoor-Imler et al. (2014), Sacks et al. (2014) and Warren et al. (2013) have estimated pollution using both monitored and modelled pollution data, by utilizing the fusion approaches proposed by Fuentes and Raftery (2005), Berrocal et al. (2010a) or McMillan et al. (2010).

This paper proposes a two-stage approach to investigate the health effects of air pollution, with inference in a Bayesian setting based on Markov chain Monte Carlo (MCMC) simulation. The first stage is a novel statistical fusion model that regresses the monitored and modelled pollution concentrations at the point-level, then makes point-level predictions of pollution across our study region, and finally aggregates these point-level predictions to the areal level required to align with the disease counts. The second stage regresses these areal level pollution summaries to the disease counts, allowing for the spatio-temporal autocorrelation in the data.

We develop our methodology for a new study investigating the long-term effects of NO₂ concentrations on respiratory disease in Scotland, UK. There have been few previous epidemiological studies of this type in Scotland, for example, only Prescott et al. (1998), Carder et al. (2008) and Willocks et al. (2012) have investigated the association between short-term exposure to air pollution and ill health, while only Lee et al. (2009) and Lee (2012) have attempted to quantify the long-term effects using an ecological spatio-temporal design. The study presented in this paper is one of the most comprehensive investigations into the effects of NO₂ concentrations on health in Scotland, as our study region is all of mainland Scotland for the five year period spanning from 2007 to 2011. In conducting this study we compare our proposed modelling approach with the simpler approach of using only the modelled concentrations, which allows us to assess the validity of using the latter in such ecological studies. We also consider whether the average (spatial mean) or the peak (spatial maximum) NO₂ concentration across each areal unit is an appropriate measure of exposure. The remainder of this paper is organised as follows. In Section 2 we describe the motivating Scotland study and present some exploratory analysis, while Section 3 proposes our new integrated pollution and health model. The results of our study are presented in Section 4, while Section 5 provides a concluding discussion.

2. Background

2.1. Data description

The study region is mainland Scotland, which is part of the United Kingdom and has a population of around 5.2 million people. Disease data have been collected for $n = 1207$ Intermediate Geographies (IG), which have an average population of around 4300 people. These data are available as yearly summaries between 2007 and 2011 inclusive, and in addition to disease prevalence data, air pollution and other covariate data such as socio-economic deprivation were collected.

The disease data are from the Scottish neighbourhood statistics database (<http://www.sns.gov.uk/>), and comprise yearly numbers of admissions to non-psychiatric and non-obstetric hospitals in each IG from 2007 to 2011 with a primary diagnosis of respiratory disease (International Classification of Disease version 10 codes J00–J99). The disease count for area k in year t is denoted by Y_{kt} , so the set of values for all n IGs in year t is denoted by $\mathbf{Y}_t = (Y_{1t}, \dots, Y_{nt})$. The number of admissions in an IG depends on its population size and demographic structure, so we adjust for this by computing the expected numbers of admissions for each IG based on its age and sex demographics. These expected disease counts are denoted by E_{kt} , and an exploratory measure of disease risk is the standardized incidence ratio (SIR), which is given by $SIR_{kt} = Y_{kt}/E_{kt}$. For example, an SIR of 1.2 corresponds to a 20% increased risk of disease compared to that expected, and a spatial map of SIR for 2011 is shown in the top left panel of Fig. 1. The figure shows that the majority of the high risk IGs are in the major cities of Glasgow and Edinburgh, which are the set of small densely populated IGs in the lower middle part of the country. This pattern in risk is largely driven by the geographical patterning in socio-economic deprivation, which needs to be controlled for in the model. Here we use two proxy measures of deprivation, namely the percentage of people living in each IG who are in receipt of Job Seekers Allowance (JSA), and the median property price in an area. The percentage of people in receipt of JSA ranges between 0.05% and 15.3% with a median value of 2.7%, while the median property price in an IG ranges between £22,800 and £500,000, with a median value of £125,000.

The pollutant considered in this study is Nitrogen Dioxide (NO₂), whose health effects have been demonstrated in the existing literature, by Ehrlich et al. (1977), Tunnicliffe et al. (1994); Lee et al. (2009). We use data on annual mean concentrations between 2006 and 2010 in this study rather than 2007–2011, ensuring the NO₂ exposure occurred before the hospital admissions. We obtained two types of NO₂ data for our study, measured concentrations at a small number of locations and modelled concentrations at a 1 kilometre (km) resolution from an atmospheric dispersion model (AEA, 2011), both as annual averages. The measured data are collected from two different devices, automatic monitors and diffusion tubes, and both data sets can be freely obtained from Air Quality in Scotland (<http://www.scottishairquality.co.uk/>). The data locations have been classified as either urban background, kerbside, roadside

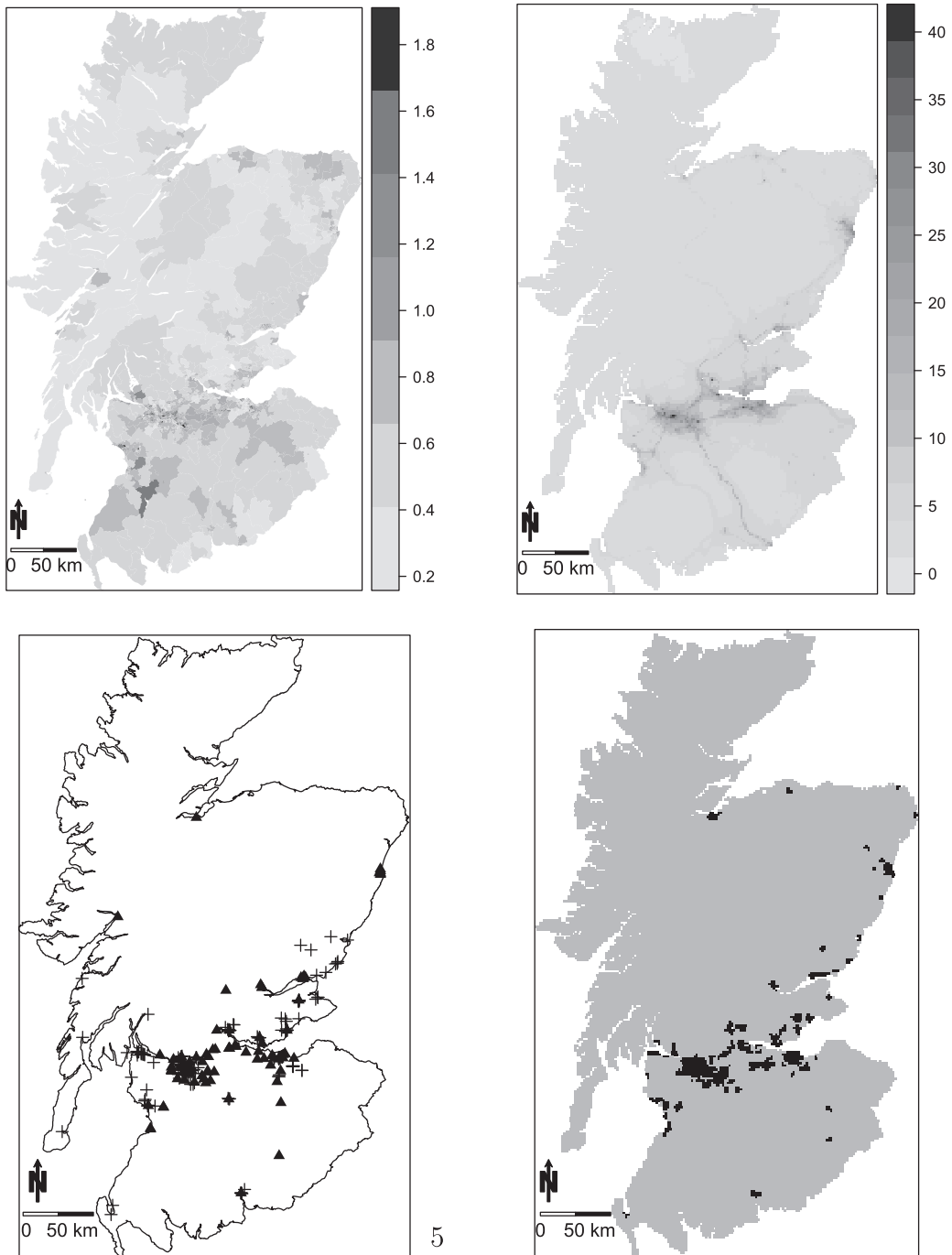


Fig. 1. Summary of the data. Top left is the SIR for respiratory disease in Scotland in 2011, top right is the DEFRA annual average NO_2 concentrations in 2010 ($\mu\text{g}\text{m}^{-3}$), bottom left is the locations of the measured NO_2 data (\blacktriangle for monitoring sites, + for tube sites), and bottom right shows mainland Scotland partitioned into urban (black) and rural areas (grey).

or rural, and a summary of the observed data is shown in Table 1. As might be expected, the pollution levels recorded at urban locations are higher than those at rural locations, and the closer the monitoring stations are to a main road, the higher the NO_2 concentrations are. The

locations of the measured data are presented in Fig. 1, which shows that they provide poor spatial coverage of Scotland as the major cities are well represented but the rest of the study region contains hardly any monitors. Therefore standard geostatistical prediction methods may

Table 1

Summary of the measured NO₂ data by site type and year: the numbers within the round brackets represent the number of sites in the form (automatic monitors, diffusion tubes), while those within square brackets indicate their corresponding mean concentrations (µgm⁻³).

Site type \ year	2006	2007	2008	2009	2010
Urban background	(3, 29) [27.3, 18.8]	(3, 29) [26.3, 18.4]	(6, 29) [27.0, 18.8]	(6, 29) [26.3, 20.1]	(6, 29) [26.0, 21.1]
Kerbside	(1, 54) [68.0, 31.5]	(4, 54) [64.0, 33.5]	(4, 54) [65.5, 31.2]	(3, 55) [67.3, 30.7]	(5, 55) [59.0, 32.4]
Roadside	(11, 94) [43.8, 33.4]	(15, 94) [42.4, 34.4]	(25, 95) [36.9, 34.4]	(30, 99) [36.2, 33.2]	(34, 99) [38.2, 34.8]
Rural	(3, 0) [8.0, NA]	(3, 0) [8.00, NA]	(3, 0) [8.33, NA]	(3, 0) [7.33, NA]	(3, 0) [9.33, NA]

not be appropriate here, due to the large distances between data locations and potential prediction locations.

As a result of this poor spatial coverage we also utilise annual mean modelled concentrations at a 1 km resolution, which are freely available and can be downloaded from the Department for Environment Food and Rural Affairs (DEFRA) database (<http://uk-air.defra.gov.uk/>), hereafter known as DEFRA concentrations. These data have complete spatial coverage of Scotland, but are known to have certain biases and needed to be calibrated to the measured data. The top right panel of Fig. 1 shows DEFRA annual average NO₂ concentrations for 2010, which exhibits a similar pattern with the spatial map of SIR for 2011, with high values in the lower middle part of the country. As temperature can affect air circulation and thus the spatial distribution of air pollution, we consider it as a covariate in our proposed pollution model outlined in Section 3. Temperature data are available as annual averages across Scotland at the 5 km resolution from the Met Office (<http://www.metoffice.gov.uk/>), and exhibit a general north–south trend as expected.

2.2. Exploratory analysis

We now present an exploratory analysis of the measured pollution data to inform our modelling approach proposed in Section 3, which aims to quantify the level of residual spatial autocorrelation remaining in these data after accounting for the known covariates. We model the measured NO₂ concentrations on the natural logarithm scale, as they are non-negative and skewed to the right and apply a simple geostatistical model to these transformed data for each year separately, where the covariates include the DEFRA concentrations (each monitoring site or diffusion tube is assigned the closest gridded DEFRA concentration) on the natural logarithm scale, the site type (e.g. roadside, rural, etc.) and temperature. The geostatistical model we fit has the form

$$\mathbf{X} \sim N(\mathbf{Z}\boldsymbol{\beta}, \Sigma = \sigma^2 \exp(-\mathbf{D}/\lambda) + \tau^2 \mathbf{I}), \quad (1)$$

where \mathbf{X} is the vector of measured NO₂ concentrations (from the automatic monitors and diffusion tubes) for a single year. The covariates are contained in the matrix \mathbf{Z} , while $\boldsymbol{\beta}$ are the associated regression parameters. The

covariance matrix is given by an exponential correlation function of distance, where \mathbf{D} is the Euclidean distance matrix between the data locations, σ^2 represents the partial sill, τ^2 is the nugget effect and λ is the spatial range parameter.

The model is fitted in the *geoR* (<http://www.r-project.org>) software in R, with inference based on maximum likelihood. The results show that the presence of residual spatial autocorrelation after accounting for the covariates is uncertain, as both the partial sill parameters (ranging between 0.059 and 0.083 for the five years of data) and the range parameters (ranging between 0.078 km and 0.924 km for the five years of data) are very small, and the empirical semi-variogram analysis suggests there is no or just very weak residual spatial autocorrelation remaining, as the empirical semi-variogram are inside or right on the border of the Monte Carlo envelopes at all distances (see e.g. Fig. 2 for 2010, and the semi-variogram plots for the other years are similar and are not shown here). This suggests that the available covariates, including the DEFRA concentrations (which themselves are spatially autocorrelated as shown in Fig. 1) have captured the majority of the spatial structure in these data, and that

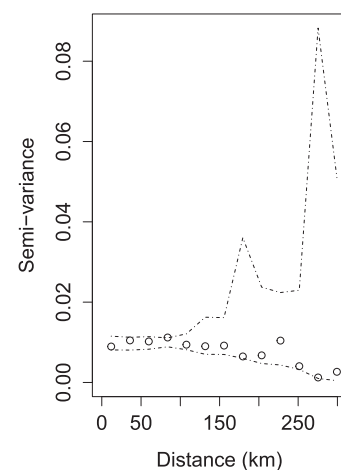


Fig. 2. The empirical semi-variogram of the residuals from the geostatistical model for 2010 (circles), with 95% Monte Carlo simulation envelopes (dashed lines).

including an additional set of spatially autocorrelated random effects is likely unnecessary.

2.3. Spatio-temporal pollution modelling

As described in Section 2.2 the pollution data contain very weak spatial autocorrelation after accounting for the covariates, and thus the spatio-temporal model proposed for the pollution data in Section 3 does not account for residual spatial autocorrelation. However, to assess the validity of this modelling approach we compare our proposed model against the spatio-temporal pollution model proposed by Sahu et al. (2007), hereafter referred to as **SGH** which does allow for residual spatial autocorrelation. The model can be implemented using the R package *spTimer* and has the general form

$$\begin{aligned} \mathbf{X}_t &= \mathbf{O}_t + \boldsymbol{\epsilon}_t \quad t = 1, \dots, T, \\ \mathbf{O}_t &= \rho \mathbf{O}_{t-1} + \mathbf{Z}_t \boldsymbol{\beta} + \boldsymbol{\eta}_t \quad t = 2, \dots, T, \end{aligned} \quad (2)$$

where \mathbf{X}_t denotes the vector of measured pollution data in year t . These noisy data are modelled as a linear combination of the true values \mathbf{O}_t and independent (white noise) errors $\boldsymbol{\epsilon}_t$. The true values are modelled with a first order autoregressive component ($\rho \mathbf{O}_{t-1}$), a regression component ($\mathbf{Z}_t \boldsymbol{\beta}$, where \mathbf{Z}_t is the t th row of \mathbf{Z} in Model (1)) and a spatial autocorrelation component $\boldsymbol{\eta}_t$. The latter is modelled independently for each time period, and is given a multivariate Gaussian prior with mean zero and an exponential correlation matrix, identical to Model (1).

3. Methodology

There are two main types of statistical fusion models developed in the literature, with the first being a regression calibration approach which regresses the measured data against the modelled concentrations via a spatially varying linear regression (see e.g. Berrocal et al., 2010a; Berrocal et al., 2010b and Berrocal et al., 2012). The second approach is to assume an underlying unknown ground truth process, which is informed separately by the monitoring data and model output (see e.g. Fuentes and Raftery, 2005; Wikle and Berliner, 2005 and McMillan et al., 2010).

In this section, we propose an integrated model for estimating the long-term health effects of air pollution, that fuses DEFRA concentrations and measured pollution data to provide improved predictions of areal level pollution concentrations. As been mentioned in Section 1, most of the existing epidemiological studies have used each of these data sources in isolation to estimate air pollution concentrations at the areal unit level, while only a few papers published recently attempted to examine the effects of air pollution on health by using fused estimates of monitored and modelled pollution data. Therefore, the present study will contribute to the extension of this literature which uses either only the measured pollution data (e.g. Janes et al., 2007; Young et al., 2009) or the modelled pollution data (e.g. Maheswaran et al., 2006; Lee et al., 2009) to estimate areal level pollution summaries. We propose a two-stage modelling approach to achieve this goal,

the first stage of which is a spatio-temporal model that produces posterior predictive distributions for pollution concentrations at the 1 km resolution in Scotland, then an aggregation step to address the different spatial supports of the pollution and disease data. The second stage estimates the health impact of air pollution using the spatially aggregated pollution summaries.

3.1. Stage 1 – air pollution model

We propose a Bayesian space-time linear regression model for relating the measured concentrations to the DEFRA concentrations, whilst allowing for additional covariate information such as site type (e.g. roadside, rural, etc.) and temperature. Our model allows for temporal autocorrelation in the model parameters in adjacent years, because annual average concentrations are unlikely to change greatly from one year to the next. Conversely, we do not assume the measured concentrations are spatially autocorrelated after accounting for the covariate effects, because the exploratory analysis in Section 2.2 provides little evidence for the presence of such autocorrelation. Let $\mathbf{X}_t = (X_t(\mathbf{s}_1), \dots, X_t(\mathbf{s}_{n_t}))$ denote the vector of n_t measured NO_2 concentrations (on the natural log scale) at sites $(\mathbf{s}_1, \dots, \mathbf{s}_{n_t})$ in year t , where $t = 1, 2, \dots, T$. These measured concentrations are related to an $n_t \times p$ design matrix of covariates \mathbf{Z}_t (including the DEFRA concentrations on the natural log scale), and the full model we propose is given by

$$\begin{aligned} \mathbf{X}_t &\sim \mathcal{N}(\mathbf{Z}_t \boldsymbol{\beta}_t, \sigma_t^2 \mathbf{I}_t) \quad t = 1, \dots, T, \\ \boldsymbol{\beta}_t &\sim \mathcal{N}(\boldsymbol{\beta} + \kappa(\boldsymbol{\beta}_{t-1} - \boldsymbol{\beta}), \tau^2 \mathbf{V}) \quad t = 2, \dots, T, \\ \boldsymbol{\beta}_1 &\sim \mathcal{N}(\boldsymbol{\beta}, \tau^2 \mathbf{V}), \\ \boldsymbol{\beta} &\sim \mathcal{N}(\mathbf{0}, 1000 \mathbf{V}), \\ \mathbf{V} &\sim \text{Inverse - Wishart}(v = p, \boldsymbol{\Psi} = 100 \mathbf{I}_{p \times p}), \\ \ln(\sigma_t^2) &\sim \mathcal{N}(\ln(\sigma_{t-1}^2), \sigma^2) \quad t = 2, \dots, T, \\ f(\ln(\sigma_1^2)) &\propto 1, \\ \kappa &\sim \text{Uniform}[0, 1], \\ \tau^2, \sigma^2 &\sim \text{Inverse - Gamma}(a = 0.001, b = 0.001). \end{aligned} \quad (3)$$

The measured pollution data in year t are modelled by a linear regression model with mean $\mathbf{Z}_t \boldsymbol{\beta}_t$ and variance $\sigma_t^2 \mathbf{I}_t$, where \mathbf{I}_t is an $n_t \times n_t$ identity matrix. The $p \times 1$ vector of regression parameters in the mean model $\boldsymbol{\beta}_t$ is assumed to be temporally autocorrelated, following a centred multivariate first order autoregressive process. The extent of this temporal dependence is captured by κ , which is assigned a uniform prior on the unit interval $[0, 1]$. If $\kappa = 0$, $\boldsymbol{\beta}_t$ is estimated independently for each year and is smoothed towards an overall mean value for all years $\boldsymbol{\beta}$, while if $\kappa = 1$, $\boldsymbol{\beta}_t$ is temporally autocorrelated with $\boldsymbol{\beta}_{t-1}$. The covariance matrix \mathbf{V} captures the potential correlations among the elements of each $\boldsymbol{\beta}_t$, and these correlations are assumed to be constant for all years. The observation variance σ_t^2 is also assumed to be temporally autocorrelated via a first order random walk prior, and as it must be non-negative, the log scale is used. Finally, we choose weakly informative conjugate prior distributions for $(\mathbf{V}, \sigma^2, \tau^2)$ by assuming them to be Inverse-Wishart and

Table 2
Simplifications of the general model (3) considered in this paper.

Model	Simplifications
1A	$\kappa = 0, \mathbf{V} = \mathbf{I}, \sigma_t^2 = \sigma^2$
1B	$\kappa = 1, \mathbf{V} = \mathbf{I}, \sigma_t^2 = \sigma^2$
1C	$\mathbf{V} = \mathbf{I}, \sigma_t^2 = \sigma^2$
1D	$\sigma_t^2 = \sigma^2$
1E	The full model

Inverse-gamma distributed respectively, where for the former $v = p$ and $\Psi = 100\mathbf{I}_{p \times p}$ as this was used by Lawson et al. (2012) as well. Inference for the collection of model parameters $\Theta = (\beta_1, \dots, \beta_T, \beta, \mathbf{V}, \kappa, \sigma_1^2, \dots, \sigma_T^2, \tau^2, \sigma^2)$ is based on MCMC simulation, using both Gibbs sampling and Metropolis–Hastings steps.

Model (3) is very general, so we compare its performance to a number of simplifications when modelling the NO₂ data in this paper to see if the full model complexity is necessary for our data. The simplifications we consider are outlined in Table 2. Model 1A is the simplest special case and assumes the elements of β_t are independent of each other and over time, and additionally the observation variance σ_t^2 is assumed to be constant in time. Models 1B and 1C are similar, and respectively assume β_t follow first order random walk and first order autoregressive processes. Model 1D allows the full generality of the mean model for β_t , but assumes the observation variance is constant, while Model 1E is the full model given by (3).

The pollution model (3) is used to predict the pollution concentrations at 1 km resolution across mainland Scotland, which results in 68,448 prediction locations for each of $T = 5$ time periods (years). For a single location \mathbf{s}_* and time period t , predictions are made from the posterior predictive distribution $f(X_t(\mathbf{s}_*)|\mathbf{X})$, where \mathbf{X} denotes the vector of measured pollution data on the natural log scale for all time periods. M predictions are made from each posterior predictive distribution via composition sampling, sampling from the distribution $N(\mathbf{Z}_{*t}^T \beta_t, \sigma_t^2 \mathbf{I}_t)$, using the equation

$$X_t^{(m)}(\mathbf{s}_*) | \Theta^{(m)} \sim N(\mathbf{Z}_{*t}^T \beta_t^{(m)}, \sigma_t^{2(m)} \mathbf{I}_t) \quad m = 1, \dots, M, \quad (4)$$

where $^{(m)}$ denotes the m th MCMC sample drawn from the posterior distribution of the model parameters and \mathbf{Z}_{*t} is the corresponding vector of covariates for the prediction location \mathbf{s}_* at time t . The posterior mean of the M exponentiated predictions (as the measured data were modelled on the natural log scale) is taken at each grid point, resulting in $Q = 68,448$ spatial point predictions $(\bar{X}_t(\mathbf{s}_{1*}), \dots, \bar{X}_t(\mathbf{s}_{Q*}))$ for each of $T = 5$ time periods. The disease data relate to irregularly shaped geographical units, and are thus spatially misaligned to the point level pollution predictions. Therefore we consider two different spatial aggregation approaches here, the spatial mean and the spatial maximum value in each areal unit. Specifically, for areal unit k and time period t we consider the following two metrics:

$$\bar{X}_{kt}^{(1)} = \frac{1}{N_k} \sum_{r \in \mathcal{A}_k} \bar{X}_t(\mathbf{s}_{r*}), \quad \bar{X}_{kt}^{(2)} = \max_{r \in \mathcal{A}_k} \{\bar{X}_t(\mathbf{s}_{r*})\}, \quad (5)$$

where \mathcal{A}_k is the set of prediction locations that fall within the k th areal unit, while N_k is the cardinality of this set. We

note that various aggregation functions for transferring spatial data into a single metric have been discussed by researchers (see e.g. Bruno and Cocchi, 2002), however, the existing literature in the context of investigating air pollution health effects uses the mean almost exclusively (e.g. Maheswaran et al., 2006; Lee et al., 2009), whereas here we investigate both metrics as it may be that peak concentrations (over space) are more correlated with disease risk than average concentrations.

3.2. Stage 2 – disease model

Recall from Section 2 that (Y_{kt}, E_{kt}) are the observed and expected numbers of disease cases in areal unit k during time period t , and the model presented here relates the pollution metrics in (5) to these disease counts whilst accounting for other covariate factors and spatio-temporal autocorrelation. The model we use was developed by Rushworth et al. (2014), and is given by:

$$\begin{aligned} Y_{kt} | E_{kt}, R_{kt} &\sim \text{Poisson}(E_{kt} R_{kt}), \\ \ln(R_{kt}) &= \mathbf{b}_{kt}^T \boldsymbol{\alpha} + \tilde{X}_{kt}^{(j)\lambda} + \phi_{kt}, \\ \boldsymbol{\alpha} &\sim N(\mathbf{0}, 1000\mathbf{I}), \\ \phi_t | \phi_{t-1} &\sim N(\gamma \phi_{t-1}, v^2 \mathbf{Q}(\rho, \mathbf{W})^{-1}), \quad t \in 2, \dots, T, \\ \phi_1 &\sim N(\mathbf{0}, v^2 \mathbf{Q}(\rho, \mathbf{W})^{-1}), \\ \lambda &\sim N(0, 1000), \\ v^2 &\sim \text{Inverse-Gamma}(a = 0.001, b = 0.001), \\ \gamma, \rho &\sim U[0, 1]. \end{aligned} \quad (6)$$

The risk of disease in areal unit k and time period t is denoted by R_{kt} , and is modelled by three components on the log-scale. The first is a vector of covariates, \mathbf{b}_{kt} such as measures of poverty, and $\boldsymbol{\alpha}$ are the corresponding regression parameters which are assigned a zero-mean Gaussian prior with a diagonal variance matrix and a large variance. The pollution metric used in this model is $\tilde{X}_{kt}^{(j)}$ from (5), where $j = 1, 2$ denotes the spatial mean and spatial maximum pollution concentration respectively. The key parameter of interest in this model is λ , the increase in the log-risk of disease for a 1 unit increase in pollution, and this is assigned a weakly informative Gaussian prior with a large variance.

The final term in the model is ϕ_{kt} , which is a random effect included to allow for any spatio-temporal autocorrelation remaining in the disease counts after the covariate effects have been accounted for. Here $\phi_t = (\phi_{1t}, \dots, \phi_{nt})$ denotes the vector of random effects for time period t , and is modelled by a multivariate first order autoregressive process with temporal autocorrelation parameter γ and variance v^2 . Spatial autocorrelation is induced into the random effects by the precision matrix, which is given by $\mathbf{Q}(\rho, \mathbf{W}) = \rho(\text{diag}(\mathbf{W}\mathbf{1}) - \mathbf{W}) + (1 - \rho)\mathbf{I}$ and corresponds to the conditional autoregressive (CAR) prior proposed by Leroux et al. (1986). Here spatial similarity is determined by a binary $n \times n$ adjacency matrix \mathbf{W} , which is based on the contiguity structure of the n areal units. In this matrix $w_{kk'} = 1$ if areal unit k shares a border with areal unit k' , otherwise $w_{kk'} = 0$, and also $w_{kk} = 0$ for all k . The level of

spatial autocorrelation in the random effects is controlled by ρ , and this can be more clearly seen by re-writing the prior for ϕ_1 in its full conditional form $f(\phi_{k1}|\phi_{-k1})$, where ϕ_{-k1} denotes the vector of random effects for time period 1 except for ϕ_{k1} . This full conditional distribution is given by

$$\phi_{k1}|\phi_{-k1} \sim N\left(\frac{\rho\sum_{i=1}^n w_{ki}\phi_{i1}}{\rho\sum_{i=1}^n w_{ki} + 1 - \rho}, \frac{v^2}{\rho\sum_{i=1}^n w_{ki} + 1 - \rho}\right), \quad (7)$$

and if $\rho = 0$ the random effects are *a-priori* independent with mean zero and a constant variance. In contrast if $\rho = 1$ the random effects are spatially autocorrelated, as the conditional expectation of ϕ_{k1} is the mean of the random effects in neighbouring areal units while the variance is inversely proportional to the number of neighbouring units. Further details about the specification of this model is given in Rushworth et al. (2014). Finally, we choose weakly informative hyperpriors for the parameters (v^2, ρ, γ) , which allows their values to be informed by the data. Inference for the collection of model parameters $\Theta = (\alpha, \lambda, \phi_1, \dots, \phi_T, v^2, \gamma, \rho)$ are based on MCMC simulation, using both Gibbs sampling and Metropolis–Hastings steps, and was implemented using the R package *CAR-BayesST* which is freely available to download from <http://cran.r-project.org>.

4. Results

We now present the results of our study investigating the long-term effects of NO₂ concentrations on respiratory hospitalisation risk in mainland Scotland between 2007 and 2011. Section 4.1 presents a validation study comparing the predictive performance of a number of different pollution models, Section 4.2 summarises the predictions from the best performing pollution model, Section 4.3 presents the estimated health effects, while Section 4.4 tests the robustness of the health associations. For all the results presented in this section, inference is achieved using MCMC simulation, where the Markov chain was burnt in for 25,000 iterations and then the next 25,000 iterations were used for the final results.

4.1. Pollution model validation

In this section we compare the predictive performance of the five variants of the air pollution model (3) proposed here and summarised in Table 2 with two alternatives, the Gaussian process model (2) (referred to as **SGH**), and simply using the DEFRA concentrations in isolation. We also validate the use of DEFRA concentrations in pollution models by running two extra pollution models without using the DEFRA concentrations as a covariate, Model 1E and Model SGH. We measure predictive performance using a 10-fold cross validation approach, where in each run we leave out 15% of the non-rural sites as a test set (only 3 rural sites are contained in the data and removing them might cause unstable prediction), and fit each model to the remaining data and predict the pollution concentrations in the test set. We quantify model performance by computing the prediction bias, root mean square predic-

Table 3

Bias, root mean square prediction error and coverage probabilities from a 10 fold cross validation exercise for the models proposed in this paper, the autoregressive Gaussian process model (**SGH**) and using only the DEFRA concentrations.

Model	Bias	RMSPE	Coverage (%)
DEFRA NO ₂	-0.7377	0.8648	-
1A	0.0250	0.3116	93.86
1B	0.0249	0.3117	93.67
1C	0.0249	0.3117	93.99
1D	0.0250	0.3124	93.80
1E	0.0259	0.3113	93.80
1E without DEFRA NO ₂	0.0158	0.3927	93.99
SGH	0.0184	0.4174	100
SGH without DEFRA NO ₂	0.0210	0.4878	100

tion error (RMSPE) and the coverage probabilities of the 95% prediction intervals. These results are presented in Table 3, and as previously discussed all models are fitted to the pollution data on the natural log scale.

The table shows a number of key results. Firstly, the five variants of the pollution model proposed here give almost identical results, with negligible bias, lower RMSPE than the other models considered and close to the nominal 95% coverage probabilities. Thus our proposed model outperforms the competitors considered here, and will be used for pollution estimation in the remainder of this section. Specifically, as Model 1A is simpler than the other variants proposed here and performs comparably, we use it for predicting pollution concentrations which being used in the disease model. The comparable performances of Models 1A and 1E for our data is because the estimated error variances σ_t^2 from the latter are very similar in each year, with posterior means of 0.096, 0.096, 0.095, 0.091, 0.089 for the five years. Furthermore, the other simplification that the covariance matrix $\mathbf{V} = \mathbf{I}$ is also not unrealistic, as the off diagonal elements of this matrix estimated from 1E are much smaller (ranging between -7.3 and 6.2) than the diagonal ones (ranging between 28.4 and 48.3).

Model **SGH** has an RMSPE that is around 24% higher than those from Models 1A to 1E, despite all models having the same covariates. This is because the spatial random effects in Model **SGH** are competing with the covariates to explain the variation in the response, resulting in attenuation in the estimated covariate effects. This is observed in Table 4, where the regression coefficients from Model **SGH** are smaller in absolute value than the corresponding estimates from Model 1A. This results in poorer prediction because the DEFRA concentrations are naturally a better predictor of the measured concentrations than a spatial random effect. Secondly, the prediction intervals from Model **SGH** are too wide with a coverage of 100%, which is likely to be because it has much larger standard deviation parameters compared with Model 1A (the observation standard deviations are 0.30 and 0.96 for Models 1A and **SGH** respectively). Table 3 also shows that using the DEFRA concentrations in isolation results in poorer spatial prediction than using both sources of data, with a RMSPE of 0.86 compared with 0.31 for the models proposed here. Finally, Table 3 shows that DEFRA concentration is an important covariate in the air pollution model as it can reduce RMSPE.

Table 4

Posterior means for the regression parameters from Model 1A and the Gaussian process model **SGH**. The five columns (β_1, \dots, β_5) are the yearly regression parameter estimates from Model 1A, while Model **SGH** has constant regression parameters over time (final column).

Parameter	β_1	β_2	β_3	β_4	β_5	SGH
Kerbside	0.577	0.580	0.569	0.568	0.576	0.294
Roadside	0.592	0.597	0.594	0.587	0.595	0.304
Rural	-0.592	-0.588	-0.587	-0.590	-0.588	-0.068
DEFRA concentrations	0.375	0.541	0.549	0.516	0.475	0.142
Datatype	0.154	0.158	0.145	0.139	0.144	-0.012
Temperature	0.078	0.091	0.082	0.069	0.073	0.052

Specifically, Model 1E without DEFRA concentrations has an RMSPE that is around 26% higher than that from Model 1E with DEFRA concentration, while this value is about 17% for Model **SGH**.

4.2. Pollution model prediction

As previously discussed the measured pollution data are classified according to their local environment, such as roadside, urban background or rural. This is likely to be an important covariate in the model, and thus we have to choose the local environment for each of our prediction locations. The set of prediction locations will be the centres of the 68,448 1 km grid squares on which the DEFRA concentrations are computed, and hence they represent the average pollution concentrations in each 1 km region. Therefore we do not specify any of the locations as roadside, as the majority of each grid square will not comprise roads (there will of course be roads in a large number of grid squares). Therefore we have to make a choice for each prediction location being urban background or rural, and for this we use the Scottish Government 8 fold Urban Rural

Classification ([The Scottish Government, 2010](#)). According to this we classify any areas with settlements of over 10,000 people as urban, while the rest are assumed to be rural, and this gives the map shown in the bottom right panel of [Fig. 1](#).

Since Model 1A performed as well as Model 1E, we use it to make pollution predictions at the 1km resolution across mainland Scotland. As described in Section 3 posterior predictive mean concentrations were computed at $Q = 68,448$ prediction locations, and were then aggregated to the IG scale using both the spatial mean and the spatial maximum (see Eq. (5)). These areal level summaries are shown in [Fig. 3](#), and will be used in the disease model in the next subsection. The Figure shows that air pollution is highest in the most densely populated cities of Glasgow and Edinburgh, in the middle (north to south) of mainland Scotland. This pattern is similar to the spatial map of DEFRA concentrations for 2010 shown in [Fig. 1](#) because the latter is naturally an important predictor of the measured data. The correlations between the DEFRA and predicted pollution concentrations are high, being 0.918 for the spatial mean across an IG and 0.885 for the spatial

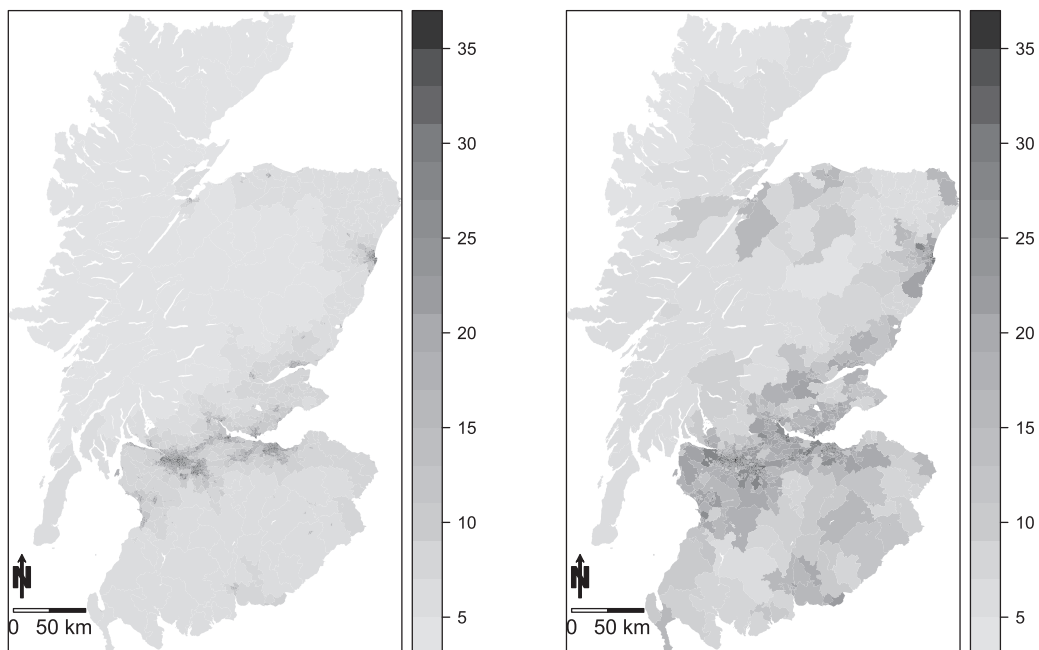


Fig. 3. Spatially aggregated predicted NO_2 concentrations from Model 1A for 2010. The left panel shows the spatial mean concentration over each IG, while the right panel shows the spatial maximum concentration over each IG.

maximum. However, the DEFRA concentrations are lower on average than the predictions from Model 1A, with the difference in the means of $5.12\mu\text{g}\text{m}^{-3}$. Additionally, the spatial mean and maximum estimates from Model 1A are highly correlated, as a Pearson's correlation coefficient between the mean and maximum concentrations across an IG is 0.884.

4.3. Disease model results

We begin by assessing the necessity of allowing for spatio-temporal autocorrelation in the disease data via the random effects in Model (6), by fitting a simplified version of that model with only known covariates. The covariates we include are mean NO_2 concentration in each IG, as well as the two proxy measures of socio-economic deprivation, namely the percentage of people in receipt of job seekers allowance (JSA) and the natural log of the median property price (Logprice). The residuals from this model show substantial spatial autocorrelation, with significant Moran's I statistics ranging between 0.254 and 0.320 over the five years. These residuals also exhibit temporal autocorrelation, as the correlation between two consecutive periods residuals are 0.659, 0.632, 0.630, 0.651 respectively (computed between the 1207 spatial data points corresponding to 1207 IGs for consecutive years). Therefore it is appropriate to include the random effects in Model (6) to allow for the spatio-temporal autocorrelation remaining in the disease counts after the covariate effects have been accounted for.

We fit four different models to the respiratory admissions data, which differ only in the NO_2 metric included in the model. Model I and II correspond to the spatial mean and maximum of the DEFRA concentrations, while Models III and IV relate to the spatial mean and maximum of the predicted pollution concentrations from Model 1A. The

results of fitting these models are displayed in Table 5, which shows that $\rho \approx 0.92$ and $\gamma \approx 0.83$ indicating high spatial and temporal autocorrelation in the disease data after the covariate effects have been accounted for, validating the use of the random effects model. These results are robust to the choice of NO_2 metric used in the model. Table 5 also shows that the covariate effects are substantial and robust across the four models, as their 95% credible intervals do not contain the null risk value of one. This indicates that the natural log of the median property price and the percentage of people receiving job seeker allowance are significantly related to hospital admissions, with a 0.38 increase in Logprice relating to 8% lower hospital admissions while a 2.35% increase in JSA results in 20% higher hospital admission rates.

Finally, Table 5 displays the long-term effects of the four metrics of NO_2 on respiratory hospitalisation risk, which are presented as relative risks for a $6.84\mu\text{g}\text{m}^{-3}$ (one standard deviation of the mean NO_2 across the 1207 IGs) increase in concentrations. The spatial maximum of DEFRA concentrations (Model II) in each IG shows a significant relationship with respiratory disease while the spatial mean of DEFRA concentrations (Model I) does not. Model II indicates that a $6.84\mu\text{g}\text{m}^{-3}$ increase in NO_2 exposure is associated with 2.3% higher respiratory disease hospital admissions in Scotland, whereas no relationship is observed when the spatial mean is used. This is similar to the work of Young et al. (2009), who found that the risk of myocardial infarction is more highly correlated with monthly maximum ozone concentrations than the average concentrations. However, as previously discussed the DEFRA concentrations are known to be biased estimates of exposure (see Table 3), but the results from Models III and IV using the pollution concentrations estimated from Model 1A validate those using the DEFRA concentrations. Specifically, the spatial maximum concentrations in Model

Table 5

Posterior means and 95% credible intervals of the regression, autocorrelation and variance parameters from fitting the disease model (6) with four different pollution metrics. Model I and II correspond to the spatial mean and maximum of the DEFRA concentrations, while Models III and IV relate to the spatial mean and maximum of the predicted pollution concentrations from Model 1A. The regression parameters are presented as relative risks for a standard deviation increase in each covariates value, which is NO_2 $6.84\mu\text{g}\text{m}^{-3}$, Logprice 0.38, JSA 2.35.

Parameter	Model I	Model II	Model III	Model IV
NO_2	1.009 (0.991, 1.028)	1.023 (1.008, 1.038)	0.993 (0.980, 1.008)	1.021 (1.004, 1.037)
Logprice	0.920 (0.910, 0.931)	0.920 (0.910, 0.929)	0.920 (0.909, 0.929)	0.921 (0.911, 0.930)
JSA	1.197 (1.181, 1.213)	1.196 (1.181, 1.212)	1.200 (1.185, 1.215)	1.196 (1.180, 1.214)
τ^2	0.061 (0.057, 0.065)	0.061 (0.056, 0.065)	0.061 (0.056, 0.065)	0.061 (0.056, 0.065)
ρ	0.917 (0.877, 0.951)	0.918 (0.879, 0.951)	0.926 (0.891, 0.956)	0.911 (0.866, 0.946)
γ	0.831 (0.795, 0.867)	0.831 (0.794, 0.867)	0.832 (0.797, 0.867)	0.830 (0.792, 0.865)

IV are associated with a significant 2.1% increased risk of disease, in comparison to a 2.3% increased disease risk using the DEFRA concentrations. Similarly, the spatial mean metric used in Models I and III show no relationship with disease risk.

4.4. Sensitivity analysis

As mentioned in Section 3.2, the flexible spatial-temporal random effects in the health model are included to account for residual auto-correlation after accounting for the effects of covariates. These flexible random effects need to compete with the explanatory ability of the NO₂ exposure. Therefore, we test the robustness of the health associations by fitting a range of generalized additive models to the data, where the random effects are replaced by smooth functions in space and time (splines) with varying levels of smoothness. Specifically, we use a linear combination of separate smooth functions for space and time, with the former being an isotropic smooth function using thin plate splines. As the data in our study contain only 5 years, the basis dimension for time can vary from 3 to 5, which actually makes little change in the smooth function and therefore is fixed at the median value 4 in the analysis. We test the robustness of the health associations against a set of different basis dimensions for the spatial smooth term, and the results are shown in Table 6. Table 6 shows that the health associations with NO₂ are robust against varying levels of control for space smoothness, as the estimates are similar to those in Table 5 regardless of the different levels of space smoothness.

5. Discussion

In this paper, we have proposed an integrated model for estimating the long-term health effects of air pollution, that fuses DEFRA and measured pollution data to provide improved predictions of areal level pollution concentrations and hence health effects. The improvement in the pollution prediction is highlighted in Table 3, which shows a 25% and a 64% decrease in RMSPE compared to using a spatio-temporal random effects model and the DEFRA concentrations respectively. The epidemiological study pre-

sented in this paper is one of the most comprehensive investigations into the effects of NO₂ concentrations on health in Scotland, as our study region is all of mainland Scotland for the five year period spanning from 2007 to 2011.

Our findings show that a 6.84 µgm⁻³ increase in peak NO₂ concentrations (spatial maximum) within an IG is associated with 2.3% higher respiratory disease hospital admissions in Scotland, while no such relationship is observed with mean concentrations (spatial mean) in an IG. This suggests that the choice of spatial aggregation metric used to quantify areal level pollution concentrations has a major impact on the resulting health effect estimate, which naturally leads to the question of which metric should one use. This issue has received little attention to date in the literature, as different exposure metrics have been used in epidemiological studies (see e.g. Basu et al., 2004; Berrocal et al., 2011). However, the majority of epidemiological studies use the average (mean) concentration (see e.g. Maheswaran et al., 2006; Lee et al., 2009; Warren et al., 2012). Therefore, in future work we will investigate this question further, and see how comparable the estimated effect sizes are for a range of spatial aggregation metrics using both real and simulated data. One key question will be whether peak concentrations regularly exhibit increased health risks compared to mean concentrations for different pollutants and study regions, or whether this result was localised to our data.

The second interesting finding of our research is the consistency between the estimated health effects of NO₂, when the latter is estimated using the DEFRA concentrations alone and both the measured and DEFRA concentrations. This consistency was observed when considering both the spatial mean and maximum as the aggregation functions, and suggests that for our data that DEFRA concentrations appear reliable to use in health effect studies despite being biased. Again future work will examine whether this result is widely true for other study regions and pollutants, or whether it is not always so consistent. This reliability of the DEFRA data is a key question, because its widespread availability makes it a popular choice for health effect studies, especially when the measured data are spatially sparse.

Table 6
Relative risk of NO₂ against various basis dimensions of the space smoothness.

Basis dimension	Model I	Model II	Model III	Model IV
$k = 30$	1.008 (1.002, 1.014)	1.023 (1.018, 1.029)	0.999 (0.994, 1.004)	1.032 (1.026, 1.038)
$k = 40$	1.009 (1.003, 1.016)	1.025 (1.019, 1.031)	0.996 (0.990, 1.001)	1.027 (1.021, 1.034)
$k = 50$	1.007 (1.000, 1.014)	1.024 (1.018, 1.030)	0.993 (0.987, 0.998)	1.026 (1.019, 1.033)
$k = 60$	1.002 (0.995, 1.009)	1.021 (1.014, 1.027)	0.989 (0.983, 0.994)	1.023 (1.016, 1.030)

There is a limitation of the design of the monitoring network in our study, where the monitor locations are highly clustered in the central part of the study region in Glasgow (west) and Edinburgh (east), and no monitors exist in large parts of the study region (see Fig. 1). Therefore, the predictive performance cannot be assessed uniformly across Scotland when we evaluated the prediction performance of several exposure models using a 10-fold cross-validation. In other words, the prediction performance at rural areas where no monitors exist is unknown. However, we note that as these areas are rural regions then NO₂ concentrations are low (away from traffic sources), so the level of uncertainty should be low and the DEFRA concentrations should be able to pick up the low background levels. This is also the key reason for using a fusion model to utilize the good spatial coverage of the DEFRA concentrations to provide estimation of pollution in these largely rural regions.

In our study the air pollution concentrations are assumed to be known and constant across each IG, by spatially aggregating predictions from our pollution model. However, these predictions are likely to contain errors and uncertainties, and in future work we will investigate these issues within our hierarchical modelling framework. A further avenue of future work could be the investigation of the individual and joint effects of different pollutants, rather than simply considering NO₂ as was the case here. Finally, it would also be of interest to extend the study by using a finer temporal scale, e.g. monthly data, so that the long-term effects of air pollution on health can be investigated with different lags between the occurrence of disease and the exposure.

Acknowledgements

The authors gratefully acknowledge the valuable comments and suggestions made by two anonymous reviewers, all of which have greatly improved the focus and content of this paper. This work is supported in part by the scholarship from China Scholarship Council (CSC) and in part by the UK Engineering and Physical Sciences Research Council (EPSRC) grant number EP/J017442/1.

References

AEA. UK modelling under the Air Quality Directive (2008/50/ec) for 2010 covering the following air quality pollutants: SO₂, NO_x, NO₂, PM₁₀, PM_{2.5}, lead, benzene, CO and ozone; 2011. <http://uk-air.defra.gov.uk/assets/documents/reports/cat09/1204301513AQD2010mapsrepmasterv0.pdf>

Basu R, Woodruff TJ, Parker JD, Saulnier L, Schoendorf KC. Comparing exposure metrics in the relationship between PM_{2.5} and birth weight in California. *J Exposure Anal Environ Epidemiol* 2004;14:391–6.

Berrocal V, Gelfand A, Holland D. A spatio-temporal downscaler for output from numerical models. *J Agric Biol Environ Stat* 2010a;15(2):176–97.

Berrocal VJ, Gelfand AE, Holland DM. A bivariate space-time downscaler under space and time misalignment. *Ann Appl Stat* 2010b;4(4):1942–75.

Berrocal V, Gelfand A, Holland D, Burke J, Miranda ML. On the use of a PM_{2.5} exposure simulator to explain birthweight. *Environmetrics* 2011;22(4):553–71.

Berrocal VJ, Gelfand AE, Holland DM. Space-time data fusion under error in computer model output: an application to modeling air quality. *Biometrics* 2012;68(3):837–48.

Besag J, York J, Mollie A. Bayesian image restoration with two applications in spatial statistics. *Ann Inst Stat Math* 1991;43:1–59.

Bruno F, Cocchi D. A unified strategy for building simple air quality indices. *Environmetrics* 2002;13(3):243–61.

Carder M, McNamee R, Beverland J, Elton R, Tongeren MV, Cohen GR, Boyd J, MacNee W, Agius RM. Interacting effects of particulate pollution and cold temperature on cardiorespiratory mortality in Scotland. *Occup Environ Med* 2008;65:197–204.

Ehrlich R, Findlay J, Fenters J, Gardner D. Health effects of short-term inhalation of nitrogen dioxide and ozone mixtures. *Environ Res* 1977;14:223–31.

Elliott P, Shaddick G, Wakefield J, de Hoogh C, Briggs D. Long-term associations of outdoor air pollution with mortality in Great Britain. *Thorax* 2007;62(12):1088–94.

Fuentes M, Raftery AE. Model evaluation and spatial interpolation by bayesian combination of observations with outputs from numerical models. *Biometrics* 2005;61(1):36–45.

Gelfand A, Zhu L, Carlin B. On the change of support problem for spatio-temporal data. *Biostatistics* 2001;2:31–45.

Gotway CA, Young LJ. Combining incompatible spatial data. *Am Stat Assoc* 2002;97(458):632–48.

Janes H, Dominici F, Zeger S. Trends in air pollution and mortality: an approach to the assessment of unmeasured confounding. *Epidemiology* 2007;18(4):416–23.

Laden F, Schwartz J, Speizer FE, Dockery DW. Reduction in fine particulate air pollution and mortality. *Am J Respir Crit Care Med* 2006;173(6):667–72.

Lawson AB, Choi J, Cai B, Hossain M, Kirby RS, Liu J. Bayesian 2-stage space-time mixture modeling with spatial misalignment of the exposure in small area health data. *J Agric Biol Environ Stat* 2012;17(3):417–41.

Lee D. Using spline models to estimate the varying health risks from air pollution across Scotland. *Stat Med* 2012;31(27):3366–78.

Lee D, Ferguson C, Mitchell R. Air pollution and health in Scotland: a multicity study. *Biostatistics* 2009;10(3):409–23.

Leroux B, Lei X, Breslow N. Spatial variation. Berlin: Springer-Verlag; 1986.

Maheswaran R, Haining R, Pearson T, Law J, Brindley P, Best N. Outdoor NO_x and stroke mortality adjusting for small area level smoking prevalence using a Bayesian approach. *Stat Methods Med Res* 2006;15:499–516.

McMillan NJ, Holland DM, Morara M, Feng J. Combining numerical model output and particulate data using bayesian space-time modeling. *Environmetrics* 2010;21(1):48–65.

Pope IC, Burnett R, Thun M, et al. Lung cancer, cardiopulmonary mortality, and long-term exposure to fine particulate air pollution. *J Am Med Assoc* 2002;287(9):1132–41.

Prescott GJ, Cohen GR, Elton RA, Fowkes FG, Agius RM. Urban air pollution and cardiopulmonary ill health: a 14.5 year time series study. *Occup Environ Med* 1998;55(10):697–704.

Rushworth A, Lee D, Mitchell R. A spatio-temporal model for estimating the long-term effects of air pollution on respiratory hospital admissions in Greater London. *Spat Spatio-Temporal Epidemiol* 2014;10:29–38.

Sacks JD, Rappold AG, Allen Davis Jr J, Richardson DB, Waller AE, Luben TJ. Influence of urbanicity and county characteristics on the association between ozone and asthma emergency department visits in north carolina. *Environ Health Perspect* 2014;122(5):506–12.

Sahu SK, Gelfand AE, Holland DM. High resolution space-time ozone modeling for assessing trends. *J Am Stat Assoc* 2007;102(480):1221–34.

The Scottish Government. Scottish Government Urban/Rural Classification 2009–2010. Scottish Government; 2010.

Tunnicliffe W, Burge P, Ayres J. Effect of domestic concentrations of nitrogen dioxide on airway responses to inhaled allergen in asthmatic patients. *Lancet* 1994;344(8939–8940):1733–6.

Vinikoor-Imler LC, Davis JA, Meyer RE, Luben TJ. Early prenatal exposure to air pollution and its associations with birth defects in a state-wide birth cohort from north carolina. *Birth Defects Res A Clin Mol Teratol* 2013;97(10):696–701.

Vinikoor-Imler LC, Davis JA, Meyer RE, Messer LC, Luben TJ. Associations between prenatal exposure to air pollution, small for gestational age, and term low birthweight in a state-wide birth cohort. *Environ Res* 2014;132:132–9.

Warren J, Fuentes M, Herring A, Langlois P. Bayesian spatial-temporal model for cardiac congenital anomalies and ambient air pollution risk assessment. *Environmetrics* 2012;23(8):673–84.

Warren J, Fuentes M, Herring A, Langlois P. Air pollution metric analysis while determining susceptible periods of pregnancy for low birth weight. *ISRN Obstetrics Gynecology* 2013;2013:1–9.

- Wikle CK, Berliner LM. Combining information across spatial scales. *Technometrics* 2005;47(1):80–91.
- Willocks L, Bhaskar A, Ramsay C, Lee D, Brewster D, Fischbacher C, Chalmers J, Morris G, Scott M. Cardiovascular disease and air pollution in scotland: no association or insufficient data and study design? *BMC Public Health* 2012;12:227.
- World Health Organisation. Ambient (outdoor) air quality and health: Fact Sheet 313; 2014. <http://www.who.int/mediacentre/factsheets/fs313/en/>
- Young LJ, Gotway CA, Yang J, Kearney G, DuClos C. Linking health and environmental data in geographical analysis: it's so much more than centroids. *Spatial Spatio-Temporal Epidemiol* 2009;1(1):73–84.